New Materials, Compounds and Applications
Vol.9, No.2, 2025, pp.362-379
https://doi.org/10.62476/nmca.92362

SYNTHESIS, CHARACTERIZATION, MOLECULAR DOCKING AND BIOLOGICAL EVALUATION OF ANILINE AND TOLIDINE DERIVATIVES AS POTENTIAL ANTI-BREAST CANCER AND ANTI-OXIDANT

Zahraa Sabah Shamkhi[1*], Kareem Salim Abbas[1], Yusra Sebri Abdul-Saheb[2]

[1]Department of Chemistry, College of Science, University of Misan, Misan, Iraq
[2]College of Pharmacy, University of Misan, Misan, Iraq

Abstract. Using p-substituted aniline and o-tolidine as starting materials, this effort involved the synthesis of many novel benzamide, sulfonamide and allyl derivatives. Benzamide derivatives (A1–A6) are prepared with 1,4-dioxane as the solvent and 4-chlorobenzoyl chloride as the reagent. In addition to the base triethylamine and the solvent dichloromethane, the reagent p-toluene sulfonyl chloride was utilized in the production of sulfonamide derivatives (B1-B5). The synthesis of allyl derivatives (C1-C3) involved the use of allyl bromide as a reagent, potassium carbonate as a base and acetone and H_2O as solvents. The identity of the synthetic compound was determined using spectroscopic methods such as FT-IR, ^{1}H-NMR, ^{13}C-NMR and mass spectroscopies, physical measurements were used to characterize all of the produced derivatives. In addition, we studied molecular docking and the biological activity of the produced derivatives, which are characterized by antioxidant and anti-breast cancer properties.

Keywords: *p-substituted aniline, allyl derivatives, antioxidant properties, anti-breast cancer properties.*

Corresponding Author: *Zahraa Sabah Shamkhi, Department of Chemistry, College of Science, University of Misan, Misan, Iraq, e-mail: zahraasabahshamhi99@gmail.com*

Received: *23 March 2025;* ***Accepted:*** *21 June 2025;* ***Published:*** *5 August 2025.*

1. Introduction

Amides a type of chemical compound have a functional group that is made up of a carbonyl group bound to a carbon on one side and a nitrogen on the other (Czerwiński & Furman, 2021). Amides have therapeutic properties and are used as antibacterial and antibiofilms (Al-Saady *et al*., 2006), antifungal (Al-Sultan *et al*., 2017) and anticancer where the directed movement of cells in response to a chemical gradient, plays a critical role in cancer metastasis (Al-Abboodi *et al*., 2011). To study this, researchers use 3D tumor spheroid models, providing a high-throughput and efficient approach to cancer treatment (AlHasan *et al*., 2013). Benzamides are significant structural components isolated from natural sources that have biological activity (Yang *et al*., 2020). For instance, molecules like proteins are vital to almost every biological action, including enzymatic catalysis (because almost all known enzymes are proteins) (Jabłońska & Tawfik, 2021), hemoglobin transport and storage, antibody defense against infection and collagen mechanical support (Falih *et al*., 2021). Because all three of the (O-C-N) chain atoms in an amide are reactive, they serve as a valuable moiety in organic compounds and are therefore essential to medicinal chemists (Sadeek *et al*., 2023). Sulfonamides are an important class of synthetic bacteriostatic (Wareham *et al*., 2024) antibiotics (Hassan,

2018) still used today for the treatment of bacterial infections and those caused by other microorganisms, a source of therapy against bacterial infections before the introduction of penicillin (Hameed *et al*., 2021). Although sulfonamides have for the most part been replaced by other agents, they still maintain considerable action in certain types of infection, for example in the urinary tract (Yaseen *et al*., 2025) and bronchitis (Hameed *et al*., 2021). The Docking program gave a distinct leap in the field of developing the preparation of therapeutic compounds especially the potential of therapeutic nanomaterials in targeting bacterial pathogens (Ali *et al*., 2022; Hussein *et al*., 2022), as after the RNA requirement for viruses and bacteria was determined (ul Qamar *et al*., 2025), it became easy to know the mechanism of dynamic association of therapeutic compounds with enzymes (Hamdoon & Saleh, 2022), proteins (Al-Abboodi *et al*., 2024), etc. N-alkylation of aniline derivatives is an important reaction in organic synthesis, which has been widely applied in the preparation of dyes (Salvatore *et al*., 2001), fluorescence probes, agrochemicals (Saleh *et al*., 2025) and pharmaceuticals. The challenge of this reaction is to obtain excellent selectivity for mono- or dialkylation products and to avoid the formation of corresponding quaternary ammonium salts (Hamdoon *et al*., 2022). There are modern catalytic reactions used to synthesize amides and sulfonamides, such as the use of carbon nanotubes and metal catalysts such as palladium and ruthenium loaded on magnetic iron for such reactions (Ali *et al*., 2023; Saleh *et al*., 2022; Saied *et al*., 2021; Saleh *et al*., 2024). Finally, this work included the preparation of substituted amides and sulfonamides, which are effective compounds that were used as anti-cancer agents and studying their association with cancer cells using the Docking program.

2. Materials and Methods

2.1. General

Chemicals compounds from Merck, BDH and Sigma. Melting points were determined by using Hot -stage, Gallen Kamp melting point apparatus uncorrected. They are measured in the Department of Chemistry College of Science, University of Misan, Iraq. At Medicine College, Misan University in Iraq, FTIR spectra were recorded using the Prestige-21. Every spectrum was captured as KBr disks. Using TMS as an internal standard and DMSO as a solvent, ^{1}H-NMR and ^{13}C-NMR spectra were performed by Bruker (model: Ultra shield 300 MHz) at the Chemistry Department of the Education College for Pure Sciences, Al-Basra University-Iraq. Agilent Technology (HP) Model 5973 is used to get mass spectra at the University of Tehran's Faculty of Science in the Islamic Republic of Iran.

2.2. Synthesis of benzamide derivatives (A1, A2,A5,A6) **(Qasim & Abbas, 2024)**

Mixed *P*-Substituted aniline (1 mmol) or o-Tolidine (0.5 mmol) and 4-chlorobenzoyl chloride (1 mmol), in a round bottom flask (25ml) With the existence of 1,4-dioxane (6 ml) as solvent, The reaction mixture was stirred at 90 °C for 12 hours used TLC (EtOAc: Petroleum ether; 1:2) until the reaction was completed. The reaction was poured over an ice bath and the resulting precipitate was filtered and purified using column chromatography (EtOAc: Petroleum ether; 1:4).

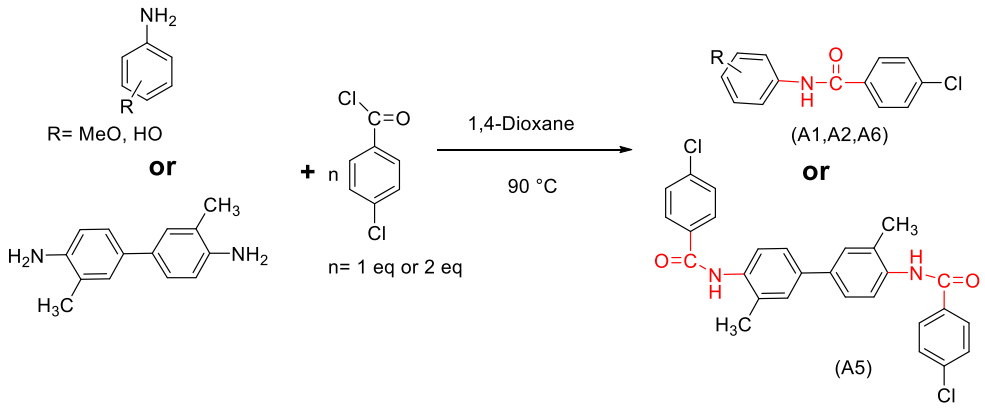

Equation 1. Synthesis of benzamide derivatives (A1, A2, A5, A6)

4-chloro-N-(4-hydroxyphenyl) benzamide A1

Light brown crystals, yield 48 %, m.p 235-237°C. FT-IR (KBr) the -OH (3435.43),-NH (3348.41), aromatic C-H (3082.37), C=O (1649.09), C=C (1614.39), C-O (1233.59), C-N (1092.04) and C-Cl (850.37)cm^{-1}.

^{1}H-NMR 10.11(-OH, s), 9.31(-NH, s), 7.97-6.74(Aromatic-H, m) ppm. ^{13}C-NMR 163.87(C=O),153.90(C-O),136.15(C-N),133.86(C-CI),129.52-115.05 (Aromatic ring) ppm.

4-chloro-N-(4-methoxyphenyl) benzamide A2

Light brown crystals, yield 52 % m.p 212-214°C. FT-IR (KBr) the -NH (3435.64), aromatic C-H (33052.00, 3095.22), aliphatic C-H (2923.72), C=O (1683.16), C=C (1592.41), C-O (1295.60), C-N (1092.53) and C-CI (762.86)cm^{-1}. ^{1}H-NMR 10.33(-NH, s), 8.00-6.93(Aromatic-H, m) 3.34 (OCH_3)ppm. ^{13}C-NMR164.21(C=O),155.89(C-O),136.47(C-N),133.96(C-CI),129.76-113.98 (Aromatic ring), 55.93(OCH_3) ppm.

N, N'-(3,3'-dimethyl-[1,1'-biphenyl]-4,4'-diyl) bis(4-chlorobenzamide) A5

Light brown crystals, yield 50 % m.p 325°C. FT-IR (KBr) the -NH (3269.19), aromatic C-H (2963.03, 2920.25), aliphatic C-H (2923.03,2853.04), C=O (1644.99), C=C (1595.39), C-O (1288.94), C-N (1016.39) and C-CI (842.44) cm^{-1}. ^{1}H-NMR 10.04 (-NH, s), 8.05-7.44(Aromatic-H, m) 2.32(CH_3, s) ppm.^{13}C-NMR164.82(C=O),

137.83(C-O),136.87(C-N),134.51(C-CI),130.12-124.62(Aromatic ring), 18.56(CH_3) ppm. MS m/z: $C_{28}H_{22}CI_2N_2O_2^+$ 488.11 found 488.7.

4-chloro-N-(4-chlorobenzoyl)-N-(4-hydroxyphenyl) benzamide A6

Light brown crystals, yield 75 %, m.p 246-248°C. FT-IR (KBr) the -OH (3438.55), aromatic C-H (3095.34, 3052.08), C=O (1682.85), C=C (1592.46), C-O (1322.24), C-N (1092.50) and C-CI (762.55). ^{1}H-NMR 13.25(-OH, s), 7.99-7.58(Aromatic-H, m) ppm. ^{13}C-NMR 163.87(C=O),153.90(C-O),138.27(C-N),130.08(C-CI),131.60-129.19 (Aromatic ring) ppm.

2.3. Synthesis of sulfonamide derivatives (B1-B5) (Rehman *et al.*, 2017)

Solved *P*-Toluene sulfonyl chloride (1.1 mmol) in (25 mL) CH_2Cl_2 at room temperature and added to the *p*-substituted aniline (1 mmol) or o-Tolidine (0.5 mmol), the mix was stirred. The resulting mixture was cooled down to 0°C before Et_3N (2.17 mmol) was slowly added. The reaction mixture was stirred for 24 hours and monitored by TLC (EtOAc: hexane; 1:1) until the reaction was completed. The layers were separated and the organic layer was extracted with water and CH_2Cl_2 dried over $MgSO_4$ and

concentrated in vacuo. The remaining residue was purified via column chromatography over silica gel using gradient elution with EtOAc and hexane (1:4) to yield sulfonamides.

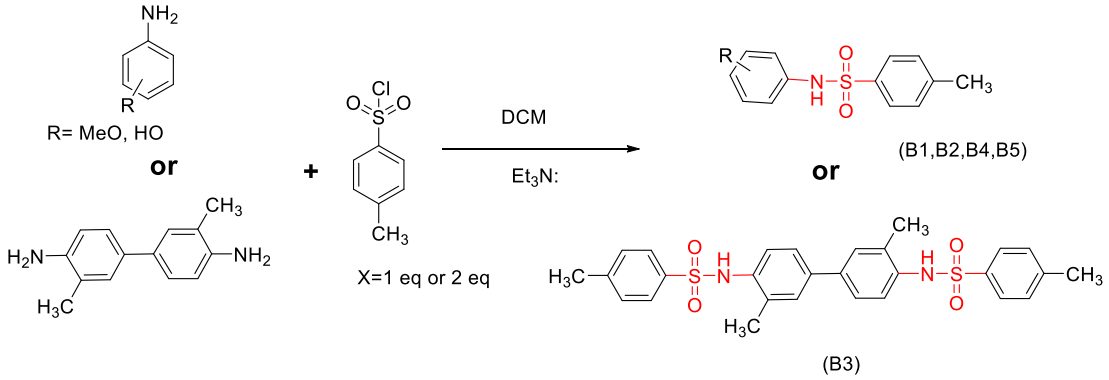

Equation 2. Synthesis of sulfonamide derivatives (B1-B5)

N-(4-hydroxyphenyl)-4-methylbenzenesulfonamide B1

White crystals, yield 55 %, m.p 129-130°C. FT-IR (KBr) -OH(3439.19), -NH(3370.38), aromatic C-H(3243.21,3065.15), Aliphatic C-H(2921.75), C=C(1506.66), S=O(1330.21), C-O(1183.80) and C-N(1093.16) cm^{-1}.

^{1}H-NMR 9.30 (-OH, s), 9.67 (-NH, s), 7.56-6.60 (Aromatic-H, m) and 2.32 (CH_3, s) ppm. ^{13}C-NMR 155.25(C-O), 137.20(C-S), 129.07(C-N), 129.92-115.98(Aromatic ring) and 21.40(CH_3) ppm.

N-(4-methoxyphenyl)-4-methylbenzenesulfonamide B2

White crystals, yield 65 %, m.p 107-109°C. FT-IR(KBr) NH(3269.68), aromatic C-H(3011.86), Aliphatic C-H(2920.25), C=C(1598.00), S=O(1396.88), C-O(1159.81) and C-N(1090.93) cm^{-1}.

^{1}H-NMR 9.87 (-NH, s), 7.58-6.78 (Aromatic-H, m), 3.66 (OCH_3, s) and 2.32 (CH_3, s) ppm. ^{13}C-NMR 196.89(C-O), 137.08(C-S), 130.70(C-N), 130.01-114.71(Aromatic ring), 55.56(OCH_3) and 21.40(CH_3) ppm.

N,N'-(3,3'-dimethyl-[1,1'-biphenyl]-4,4'-diyl)bis(4-methylbenzenesulfonamide) B3

White crystals, yield 40 %, m.p 133°C. FT-IR(KBr) NH(3437.45,3286.05), aromatic C-H(3030.50), Aliphatic C-H(2853.01), C=C(1598.55), S=O(1490.99), C-O(1163.47) and C-N(1092.45) cm^{-1}.

^{1}H-NMR 9.57 (-NH, s), 7.67-7.39 (Aromatic-H, m) and 2.36-2.02(CH_3, s) ppm. ^{13}C-NMR, 137.37(C-S), 134.76(C-N), 134.70-124.77(Aromatic ring) and 21.65-21.44(CH_3) ppm. MS m/z: $C_{28}H_{28}N_2O_4S_2^+$ 520.15 found 520.4.

N-(4-hydroxyphenyl)-4-methyl-N-tosylbenzenesulfonamide B4

White crystals, yield 75 %, m.p 175°C. FT-IR(KBr) OH(3242.34), aromatic C-H(3062.96), Aliphatic C-H(2988.16), C=C(1598.99), S=O(1460.11), C-O(1199.72) and C-N(1091.71) cm^{-1}.

^{1}H-NMR 14.75 (-OH, s), 7.99-7.20 (Aromatic-H, m) and 2.35(CH_3, s) ppm. ^{13}C-NMR,148.37(C-O) 138.41(C-S), 145.79(C-N), 132.01-115.10(Aromatic ring) and 21.62(CH_3) ppm.

N-(4-hydroxyphenyl)-4-methyl-N-tosylbenzenesulfonamide B5

White crystals, yield 27 %, m.p 164°C. FT-IR(KBr), aromatic C-H (3030.17), Aliphatic C-H (2839.22), C=C (1510.26), S=O (1465.90), C-O (1161.15) and C-N (1091.71) cm^{-1}.

^{1}H-NMR 7.70-6.88 (Aromatic-H, m), 3.78 (OCH_3, s) and 2.45(CH_3, s) ppm. ^{13}C-NMR,160.90(C-O) 136.70(C-S), 145.78(C-N), 133.01-115.10(Aromatic ring), 55.97(OCH_3) and 21.65(CH_3) ppm.

2.4. Synthesis of N- allyl derivatives (C1-C3) (Tanaka *et al*., 2009)

A mixture of (A1, A6 (2.1 mmol)) or *o*-Tolidine (1.05 mmol), Allyl bromide (2.4 mmol) and K_2CO_3 (4.4 mmol) in acetone (20 mL) and H_2O (3 mL) was stirred for 6 hours at room temperature. The reaction progress was monitored by TLC (EtOAc: Petroleum ether; 1:3) until the reaction was completed. The reaction mixture was diluted with EtOAc (50 mL), washed with brine (3 × 10 mL), dried over $MgSO_4$, evaporated under reduced pressure by rotary evaporator and the product was purified via silica gel chromatography using (EtOAc: Petroleum ether; 1:9) as eluent to give the product as a solid in excellent purity.

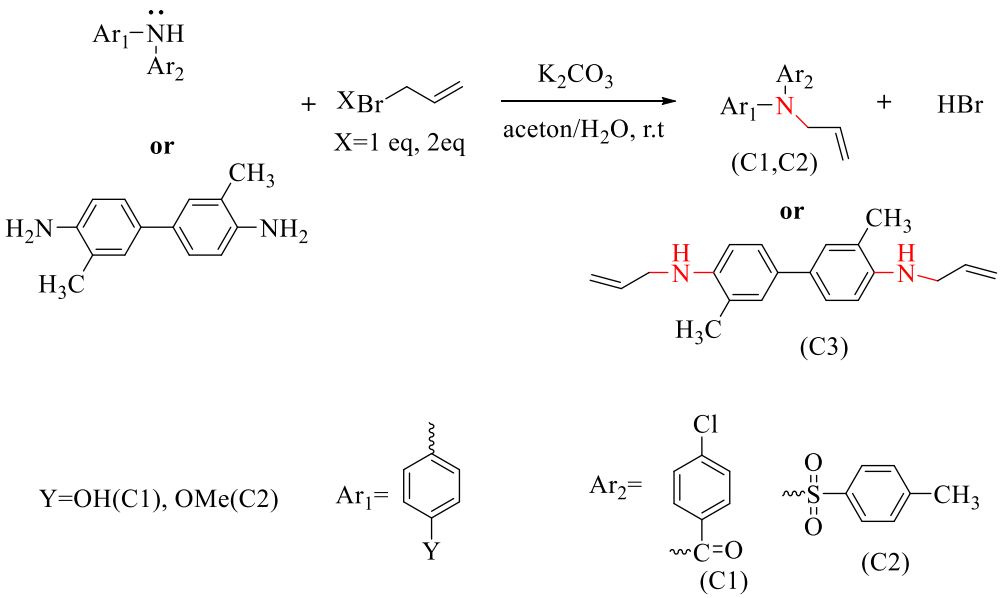

Equation 3. Synthesis of allyl derivatives (C1-C3)

N-allyl-4-chloro-N-(4-hydroxyphenyl) benzamide C1

Light yellow crystals, yield 75 %, m.p 177-179°C. FT-IR(KBr), -OH(3436.11), aromatic C-H(2921.19), Aliphatic C-H(285216), C=O(1648.44), C=C(1538.61), C-O(1253.35), C-N(1096.07) and C-CI(822.13)cm^{-1}. ^{1}H-NMR 10.22 (-OH, s), 7.99-6.64 (Aromatic-H, m), 6.07-6.01(-CH, m),5.42-5.25(=CH_2, dd) and 4.56-4.54(-CH_2,d) ppm.

^{13}C-NMR 164.45(C=O),155.01(C-O), 136.69(C-CI), 134.18(C-N), 129.99-115.03(Aromatic ring),132.61(-CH), 117.83(=CH_2), 68.77(-CH_2) ppm. MS m/z: $C_{16}H_{14}CINO_2^+$ 287.4 found 287.4

N-allyl-N-(4-methoxyphenyl)-4-methylbenzenesulfonamide C2

Light yellow crystals, yield 60 %, Oily. FT-IR(KBr), aromatic C-H (3066.82), Aliphatic C-H (2841.15), C=O(1600.92), C=C(1460.01), C-O(1249.87) and C-

N(1089.78)cm^{-1}. ^{1}H-NMR 7.48-6.85 (Aromatic-H, m), 5.68-5.63(-CH, m),5.13-5.02(=CH_2, dd) and 4.56-4.13(-CH_2, d) ppm.

^{13}C-NMR158.86(C-O) ,131.60(C-N) ,130.26-114.45(Aromatic ring), 133.62(-CH), 119.14(=CH_2), 53.41(-CH_2)ppm.

N4, N4'-diallyl-3,3'-dimethyl-[1,1'-biphenyl]-4,4'-diamine C3

Light yellow crystals, yield 30 %, Oily. FT-IR(KBr),-NH(3431.36),aromatic C-H (3074.53), Aliphatic C-H (3074.53), C=C (1612.49) and C-N(1070.49)cm^{-1}. ^{1}H-NMR 7.33 (-NH, s), 7.41-7.06 (Aromatic-H, m), 5.81-5.76(-CH, m),5.21-5.09(=CH_2, dd) and 3.58-3.57(-CH_2, d)ppm.^{13}C-NMR158.86(C-O),131.60(C-N),130.26-114.45(Aromatic ring), 133.62(-CH), 119.14(=CH_2), 53.41(-CH_2),21.51(CH_3) ppm.

MS m/z: $C_{20}H_{24}N_2^+$ 292.19 found 291.3.

Table 1. Some physical properties of the prepared compounds

Comp. No.	Structural formula	Molecular Formula	Yield (%)	M.P (°C)	Molecular Weight
A1	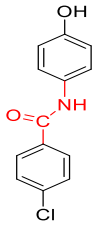	$C_{13}H_{10}O_2ClN$	48	235-237	247.04
A2	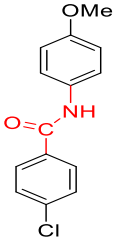	$C_{14}H_{12}O_2ClN$	52	212-214	261.06
A5	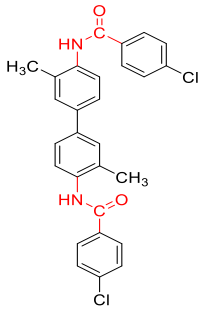	$C_{28}H_{22}O_2Cl_2N_2$	50	325	489.40
A6	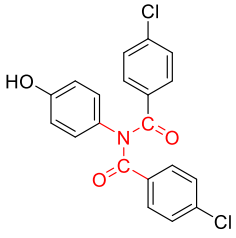	$C_{20}H_{13}O_3Cl_2N$	75	246-248	386.23

B1	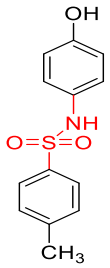	$C_{13}H_{13}O_3NS$	55	129-130	263.31
B2	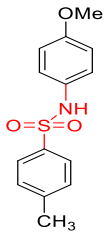	$C_{14}H_{15}O_3NS$	65	107-109	277.34
B3	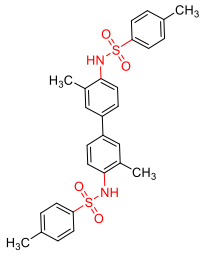	$C_{28}H_{28}O_4N_2S_2$	40	133	520.66
B4	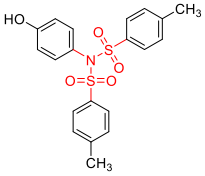	$C_{20}H_{19}O_5NS_2$	75	175	417.07
B5	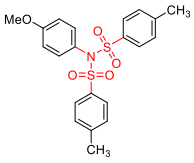	$C_{21}H_{21}O_5NS_2$	27	164	431.52
C1	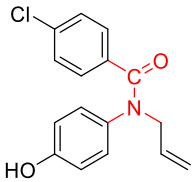	$C_{16}H_{14}O_2ClN$	75	177-179	387.74
C2	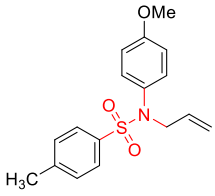	$C_{17}H_{19}O_3NS$	60	oily	317.40

C3	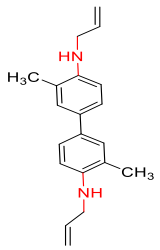	$C_{20}H_{24}N_2$	30	oily	292.43

3. Biological activity

3.1. Biological activity by In silico

Program MOE 2015 was employed to analyze the capacity of compounds to inhibit breast cancer by coupling them with a single protein (PDB: 3eqm). Table 2 shows that the prepared compounds showed good activity against the studied protein and some of them (highlighted in yellow) were selected for in vitro study (Tanaka *et al*., 2009; El-Bindary *et al*., 2020).

Table 2. Molecular docking for anti-cancer of the prepared derivatives

Compound (Ligands)	Target protein: Oxidoreductase (3EQM)						
	E Binding (Kcal/mol)	RMSD	Position of interaction		Interaction	Distance (Aº)	E (Kcal/mol)
			Ligand	Receptor			
A1	-7.0946	1.0495	O (7) O (10) CI (17) 6-ring	O (PRO 429) SD (MET311) SD (MET303) CA (GLY 439)	H-donor H-donor H-donor Pi-H	3.21 3.68 3.80 4.16	- 0.8 - 0.9 - 0.7 - 1.0
A2	-7.7234	1.1507	CI (16) 6-ring	NH_2 (ARG115 CB (CYS 437)	H-acceptor Pi-H	3.20 4.35	-0.9 -0.6
A5	-7.1083	1.4817	O (20) 6-ring 6-ring	SG (CYS 437) CA (VAL 373) CB (ALA 438)	H-donor Pi-H Pi-H	3.52 4.72 3.93	-1.4 -0.6 -0.6
A6	-8.4791	2.3946	CI (26) CI (25)	SD (MET 447) NH_2 (ARG 375)	H-donor H-acceptor	3.76 3.51	-0.2 -0.8
B1	-7.2851	2.5686	O (11)	N (MET 374)	H-acceptor	3.22	-1.8
B2	-7.3495	1.7967	O (9) O (10) 6-ring	N (ALA 438) NH_2 (ARG 115) CB (CYS 437)	H-acceptor H-acceptor Pi-H	3.52 3.11 3.86	-0.6 -0.8 -0.6
B3	-10.3703	1.4371	N (14) O (19) O (20) O (22)	OG1 (THR 310) SD (MET 311) SG (CYS 437) CA (VAL 373)	H-donor H-donor H-donor H-acceptor	2.73 3.08 3.14 3.44	-4.1 1.1 0.4 -0.7
B4	-8.8628	3.2356	6-ring 6-ring	CB (ALA 306) CB (CYS 437)	Pi-H Pi-H	4.18 3.81	-0.7 -0.9
B5	-9.2270	1.0951	O (19) O (20) 6-ring 6-ring	CA (CYS 437) NH_2 (ARG 115) CA (VAL 373) CB (ALA 438)	H-acceptor H-acceptor Pi-H Pi-H	3.35 2.95 4.69 4.04	-0.8 -1.5 -0.6 -0.9
C1	-7.2247	1.2386	O (10) 6-ring 6-ring	N (GLY 439) CB (ALA 306) N (ALA 438)	H-acceptor Pi-H Pi-H	2.82 3.83 4.20	-4.0 -0.7 -0.7
C2	-8.4408	0.8845	6-ring 6-ring	CG1 (ILE 133) N (ALA 438)	Pi-H Pi-H	3.94 4.49	-0.7 -0.9
C3	-9.8786	0.7349	6-ring	CA (GLY 439)	Pi-H	4.56	-0.6

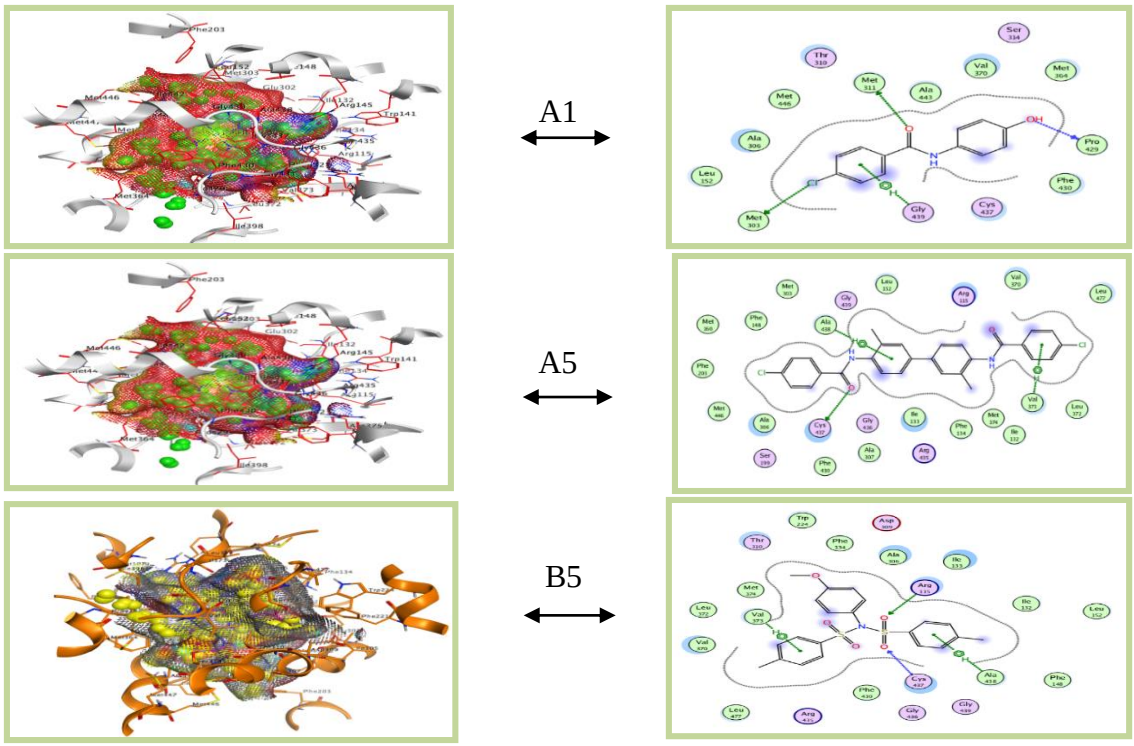

Figure 1. The interaction mode of compounds (A1, A3, A9) with active site amino acids of the protein (PDB 3EQM)

3.2. The cytotoxic activity of (A1, A2, A5, B4, B5) against human breast cancer cells line (MCF-7) in Vitro Using MTT Assay

In widely used, the concept of IC_{50} is perceived as an inhibition efficiency indicator of a biological and biochemical material in the pharmaceutical field and its value shows the inhibitory concentration required to halve a specific biological substance or biochemical function (Liu *et al*., 2018). The high IC_{50} values indicate low inhibitory activity with the material in contrast to the materials with low IC_{50} values. In this study, the MCF-7 cell line was used to assay the antiproliferative activity of different compounds. The cytotoxic impact of (A1, A2, A5, B4, B5) on the breast cancer cell line (MCF-7) was determined using the 3-(dimethylthiazol-2-yl)-2,5-diphenyltetrazolium bromide (MTT) assay. Using different compound concentrations, the MTT Assay was conducted to determine the cell viability and inhibition rate on the tumor cell line (Ahmad *et al*., 2024; Neubig *et al*., 2003). The cytotoxic effect of (A1, A2, A5, B4, B5) in concentration ranged from (7.4-600) µg/ml on MDA-MB-231 cells. Table (3) presented a decrease in cell viability in a dose-dependent pattern. The cell viability is reduced by increasing the concentration of (A1, A2, A5, B4, B5). The compound B4 exhibited significantly the most potent cytotoxic activity with good values (47.39 µg/mL) of IC50 for the MDA-MB-231 cells line, Figure 3. Conversely, compound A2 was the lowest in potency with an IC_{50} value of 8112.57 µg/mL, Figure 3. Most of the synthesized compounds (**A1, A2, A5, B4, B5)** exhibited cytotoxic activity against MCF-7 cell lines with IC50 value in the range of (47.39-8112.57 µg/mL).

Table 3. Growth inhibition percentages of breast cancer against different concentrations of the studied compounds

Sample ID	B4								MCF7 24h	
Concentration (µg/ml)	7.4		22.22		66.66		200		600	
absorption at 570 nm	0.769	0.710	0.641	0.655	0.447	0.478	0.348	0.306	0.201	0.148
Viability (%)	92.54	85.44	77.14	78.82	53.79	57.52	41.88	36.82	24.19	17.81
Average Viability (%)	88.99		77.98		55.66		39.35		21.00	
Standard Deviation (±)	5.02		1.19		2.64		3.57		4.51	

Sample ID	A2								MCF7 24h	
Concentration (µg/ml)	7.4		22.22		66.66		200		600	
absorption at 570 nm	0.825	0.829	0.810	0.793	0.767	0.759	0.652	0.682	0.540	0.550
Viability (%)	99.28	99.76	97.47	95.43	92.30	91.34	78.46	82.07	64.98	66.19
Average Viability (%)	99.52		96.45		91.82		80.26		65.58	
Standard Deviation (±)	0.34		1.45		0.68		2.55		0.85	

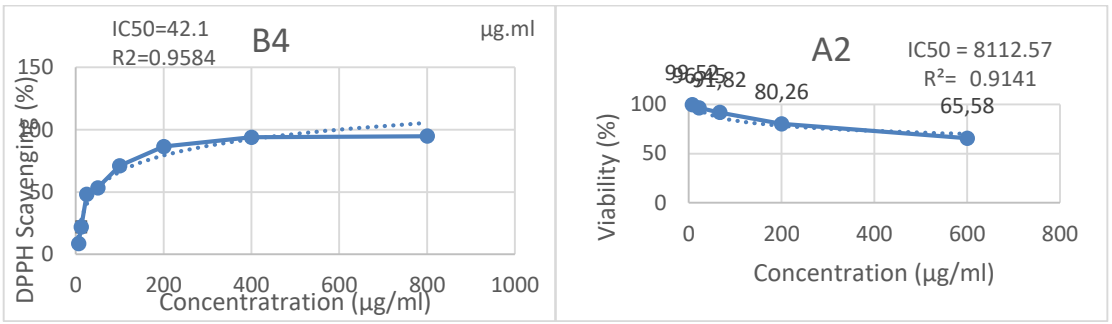

Figure 3. The Values of IC50 for synthesis compounds against MCF-7 Cell line

(A). MCF-7 cell lines treated with A2 inhibition activity 7.4 µg/mL

(B). MCF-7 cell lines treated with A2 inhibition activity 22.22 µg/mL

(C). MCF-7 cell lines treated with A2 inhibition activity 66.66 µg/mL

(D). MCF-7 cell lines treated with A2 inhibition activity 200 µg/mL

(E). MCF-7 cell lines treated with A2 inhibition activity 600 µg/mL

(A). MCF-7 cell lines treated with A2 inhibition activity 7.4 µg/mL

(B). MCF-7 cell lines treated with A2 inhibition activity 22.22 µg/mL

(C). MCF-7 cell lines treated with A2 inhibition activity 66.66 µg/mL

(D). MCF-7 cell lines treated with A2 inhibition activity 200 µg/mL

(E). MCF-7 cell lines treated with A2 inhibition activity 600 µg/mL

3.3. Antioxidant activity of the DPPH scavenging assay

This assay is a rapid, simple and vastly used method to measure the ability of compounds to act as free radical scavengers or hydrogen donors. After abstracting hydrogen from the corresponding donor, the radical loses its characteristic deep violet color and turns to yellow. The IC50 values were used to compare the antiradical scavenging activity of different analyzed samples with those of standard antioxidant compounds. The IC50 values cleared that the **A1** compound exhibited the highest antiradical scavenging activity with the lowest IC50 value (6.9 µg/mL), while the **A2** had the lowest capacity to scavenge the radical with the highest IC50 value (31019.2 µg/mL). Antioxidant drugs facilitate the conversion of DPPH into a stable diamagnetic molecule (Ali *et al*., 2025), DPPH, by electron or hydrogen transfers. A change in the color from purple to yellow signifies an increase in the radical scavenging activity of the compounds being examined. The capacity of DPPH radicals to be reduced was assessed by quantifying the decrease in absorbance at 515 nm resulting from the presence of antioxidants (Sterle *et al*., 2023). However, it is commonly recognized that organic compounds with electron-donating groups such as amine and methoxy (Baliyan *et al*., 2022) can function as agents that scavenge free radicals given the potential role of oxidative stress in cancer progression (Lawi *et al*., 2021), future studies could investigate the antioxidant properties of these compounds. The results of the antioxidant activity test with DPPH were expressed as % inhibition (Table 4), which was then linked to a series of samples or standard concentrations to produce a curve.

Table 4. Free radical scavenging activity result of synthesis compounds

Compounds	Radical Scavenging Activity % (RSA) at eight different concentrations (µg/mL)							
	800	**400**	**200**	**100**	**50**	**25**	**12.4**	**6.25**
A1	86.8	80.9	73.3	65.6	63.2	62.3	59.7	45.5
A2	4.5	3.3	2.9	2.7	2.1	1.1	0.8	0.2
B4	94.8	93.9	86.5	71.0	53.3	48.2	21.9	8.6
B5	30.0	28.7	26.8	21.9	20.5	20.1	14.5	15.2
A5	34.8	31.1	27.9	20.4	17.7	15.4	10.1	10.5

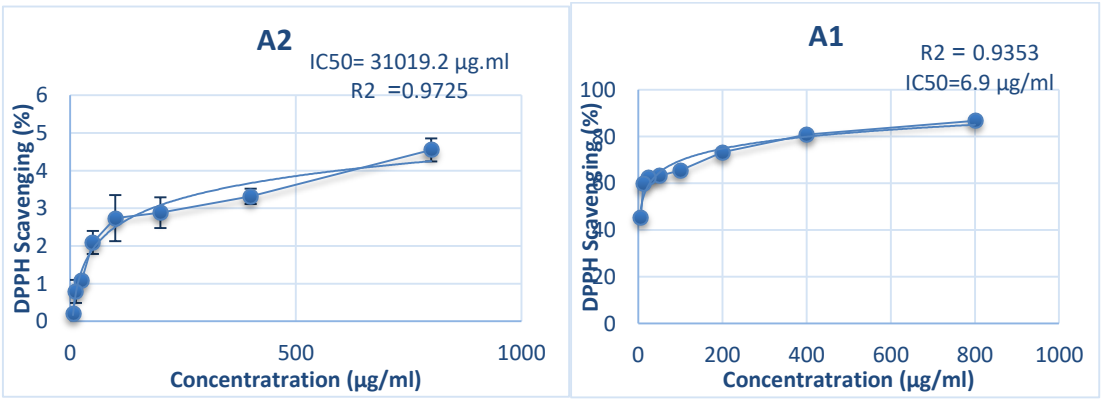

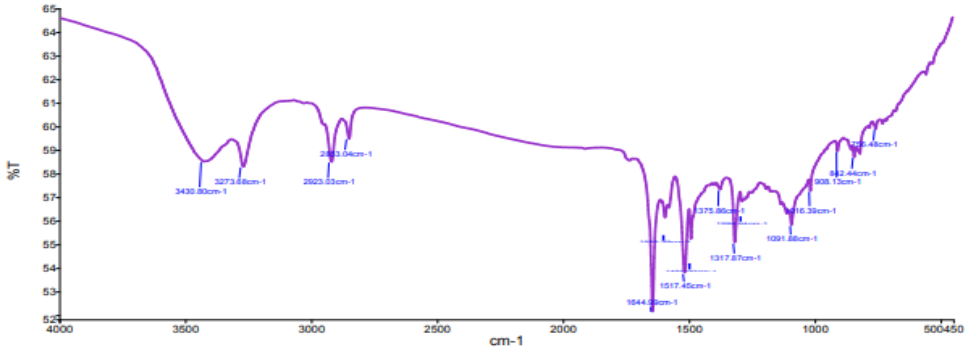

Figure 4. FT-IR spectrum of the compound A5

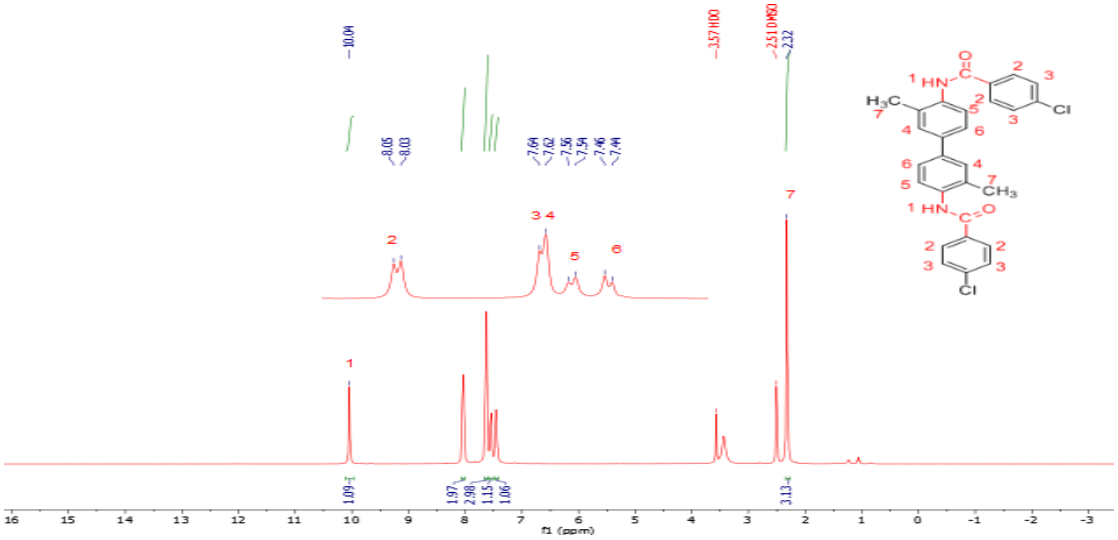

Figure 5. [1]H-NMR Spectrum of the compound A5

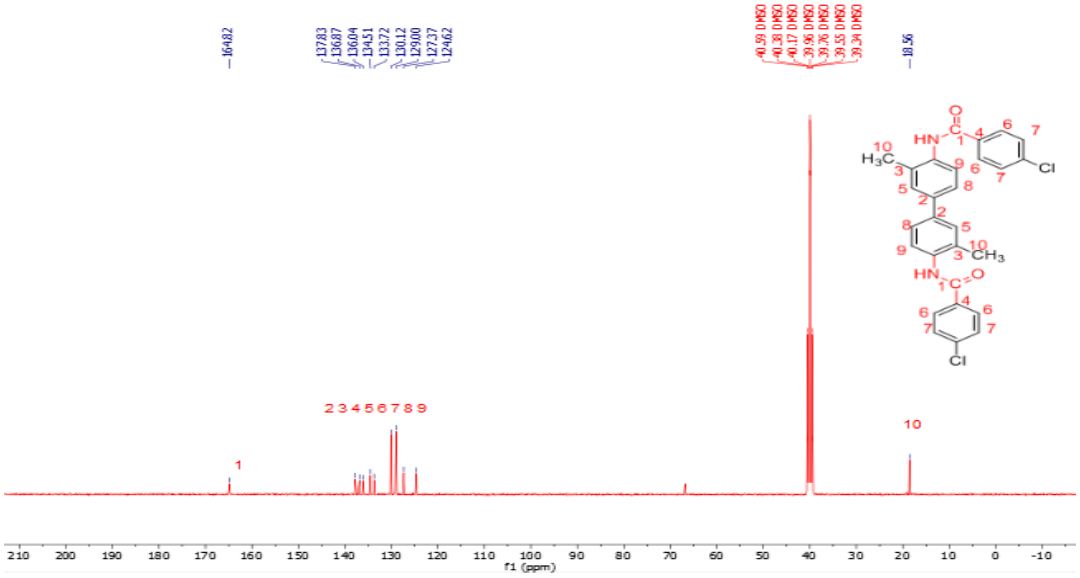

Figure 6. [13]**C**-NMR Spectrum of the compound A5

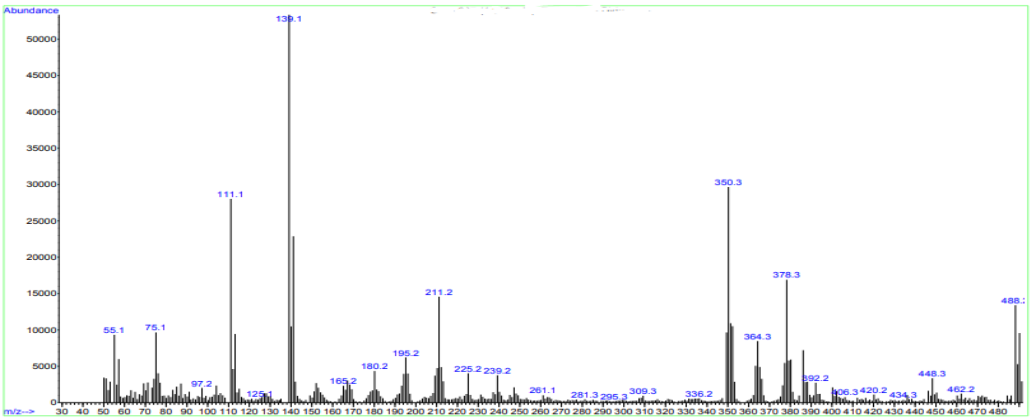

Figure 7. Mass spectrum of A5

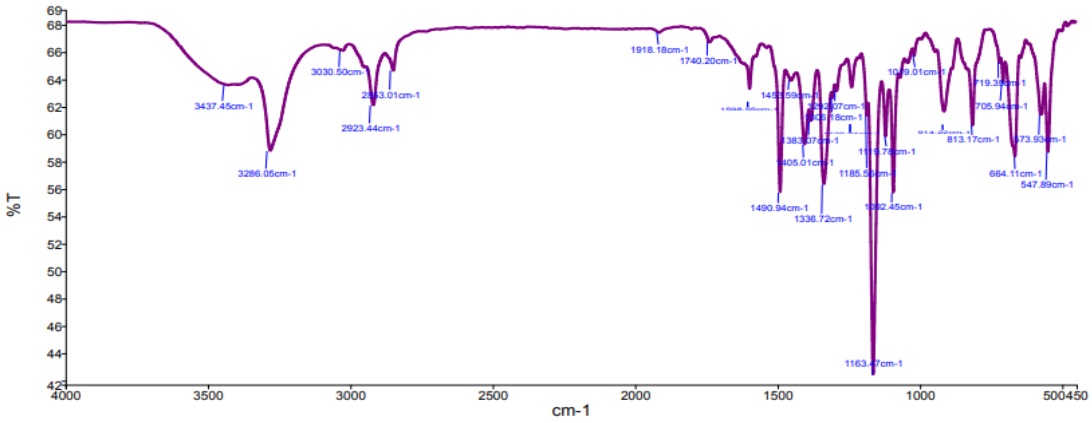

Figure 8. FT-IR spectrum of the compound B3

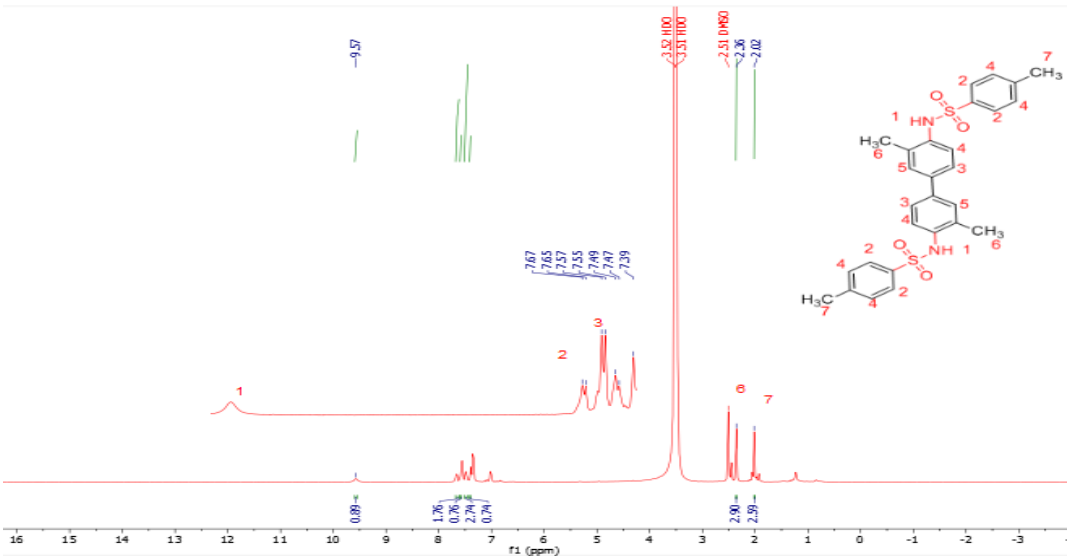

Figure 9. ^{1}H-NMR Spectrum of the compound B3

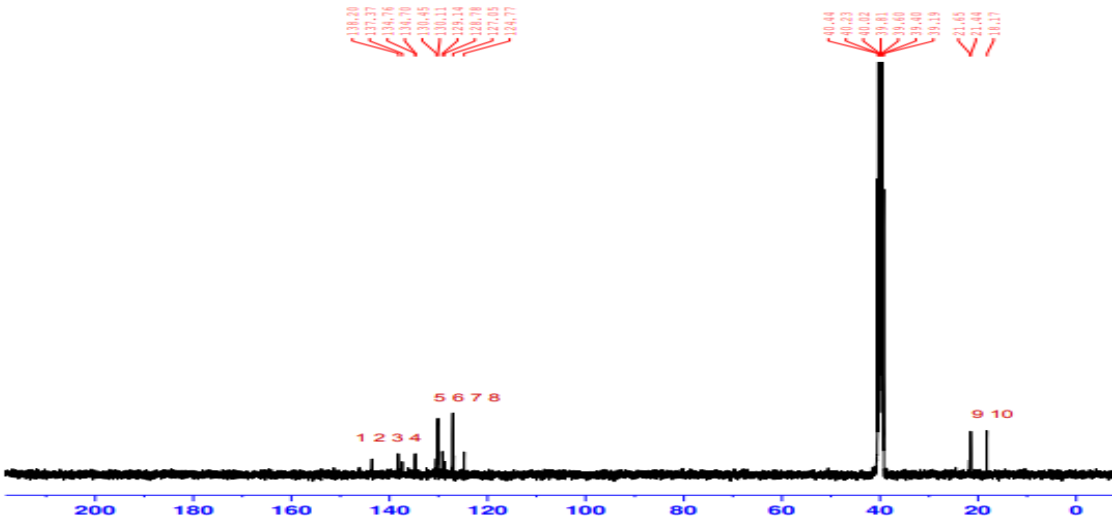

Figure 10. ^{13}C-NMR Spectrum of the compound B3

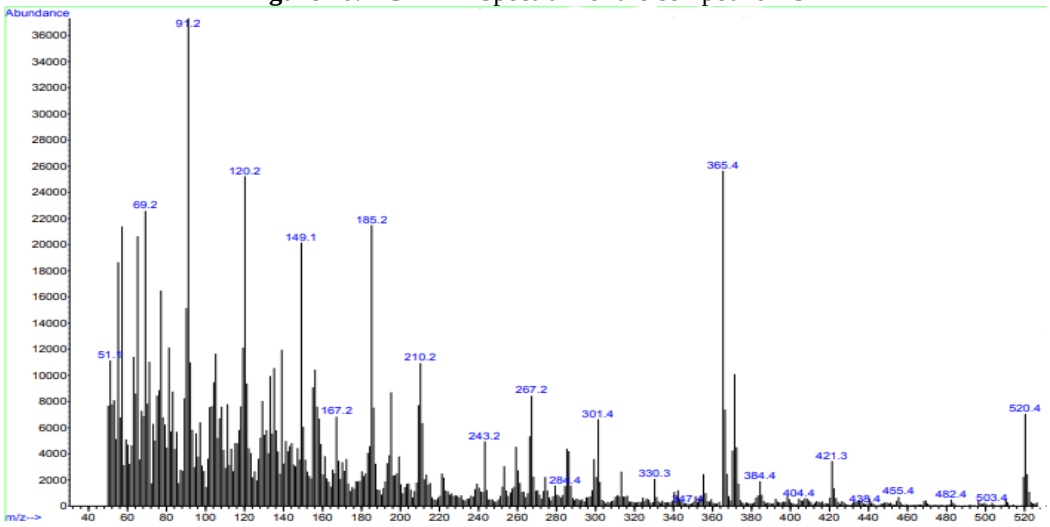

Figure 11. Mass spectrum of B3

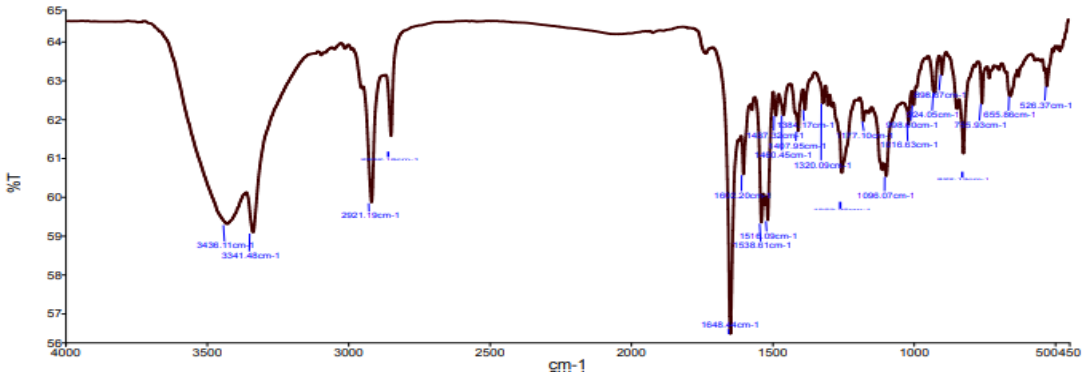

Figure 12: FT-IR spectrum of the compound (C1)

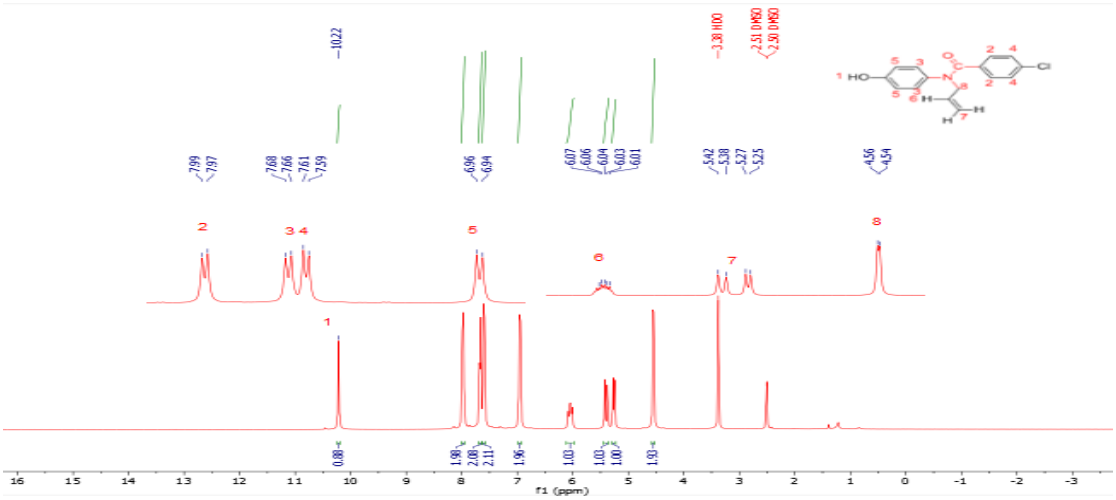

Figure 13. ^{1}H-NMR Spectrum of the compound C1

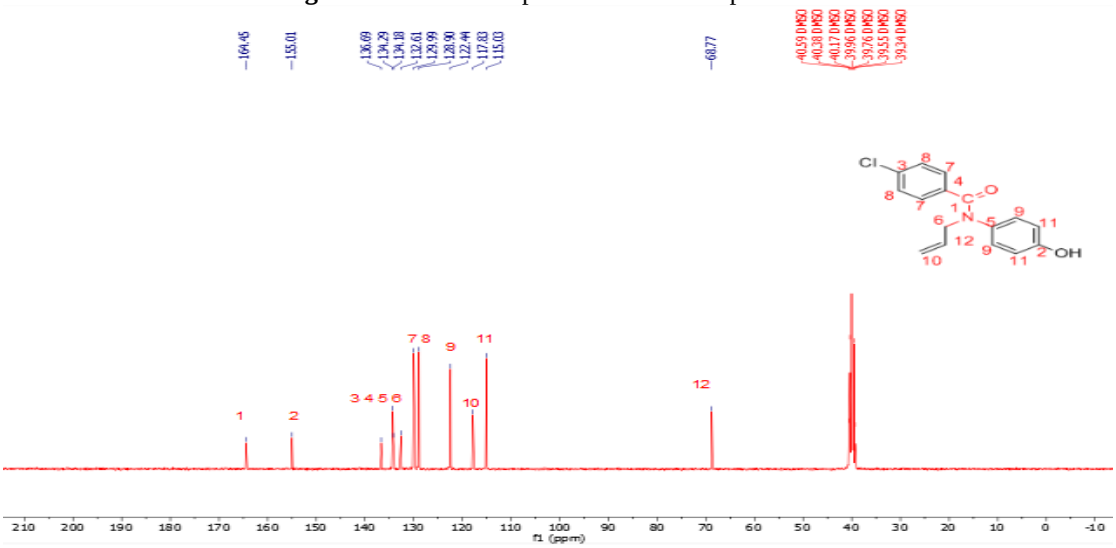

Figure 14. ^{13}C-NMR Spectrum of the compound C1

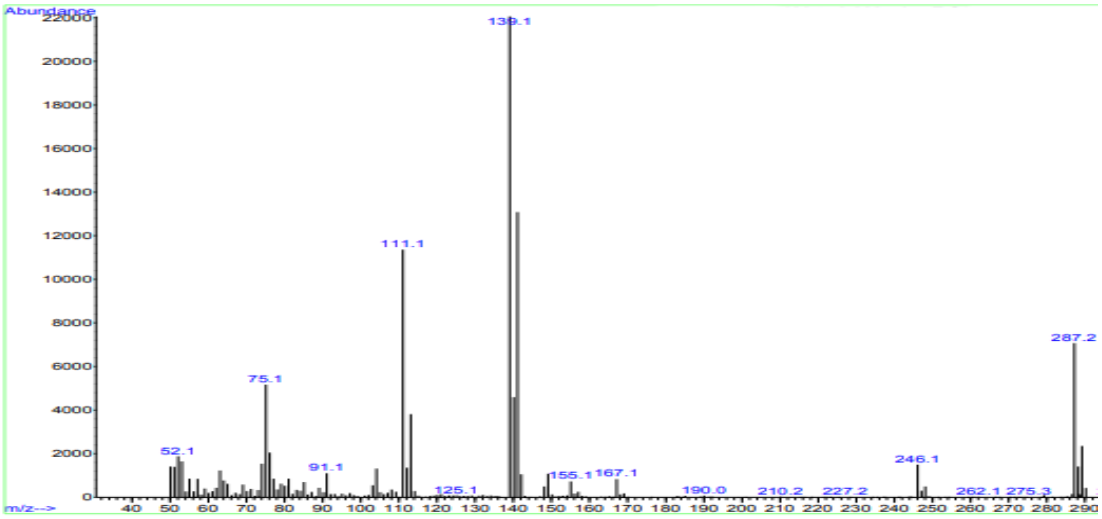

Figure 15. Mass spectrum of (C1)

4. Conclusion

The molecular docking analysis revealed promising interactions between the synthesized derivatives and breast cancer target proteins, suggesting their potential as anticancer agents. Furthermore, the in vitro cytotoxicity assessment demonstrated the effectiveness of selected compounds, with compound B4 showing the most significant antiproliferative activity against MCF-7 breast cancer cell lines.

Additionally, the antioxidant activity evaluation using the DPPH scavenging assay highlighted the strong radical-scavenging potential of specific derivatives, particularly A1, which exhibited the highest antioxidant capacity. These findings emphasize the dual therapeutic potential of the synthesized compounds as anticancer and antioxidant agents. Future research should focus on further in vivo studies, mechanistic investigations and potential clinical applications to develop these compounds into viable therapeutic candidates.

References

Ahmad, H.M., Aldahham, B.J. & Saleh, M.Y. (2024). Dehydroepiandrosterone supplementation improves diminished ovarian reserve clinical and in silico studies. *Steroids*, 211, 109490.

Al-Abboodi, A., Albukhaty, S., Sulaiman, G.M., Al-Saady, M.A., Jabir, M.S. & Abomughaid, M.M. (2024). Protein conjugated superparamagnetic iron oxide nanoparticles for efficient vaccine delivery systems. *Plasmonics*, *19*(1), 379-388.

Al-Abboodi, A., Tjeung, R., Doran, P., Yeo, L., Friend, J. & Chan, P. (2011). Microfluidic chip containing porous gradient for chemotaxis study. In *Smart Nano-Micro Materials and Devices*, 8204, 219-224. SPIE.

AlHasan, L., Qi, A., Al-Aboodi, A., Rezk, A., Shilton, R.R., Chan, P.P., ... & Yeo, L. (2013). Surface acoustic streaming in microfluidic system for rapid multicellular tumor spheroids generation. In *Micro/Nano Materials, Devices and Systems*, 8923, 828-831.

Ali, A.H., Saleh, M.Y. & Owaid, K.A. (2023). Mild synthesis, characterization and application of some polythioester polymers catalyzed by cetrimide ionic liquid as a green and eco-friendly phase-transfer catalyst. *Iranian Journal of Catalysis*, *13*(1).

Ali, A.H., Saleh, M.Y., Yaqoob, Q.A., Saied, S.M., Hasan, M.S., Owaid, K.A., ... & Alsirhani, A.M. (2025). Comprehensive evaluation of antibacterial and anticancer activities from indole butanoic acid. *Journal of Genetic Engineering and Biotechnology*, *23*(1), 100452.

Ali, Z.H., Al-Saady, M.A.A.J., Aldujaili, N.H., Rabeea Banoon, S. & Abboodi, A. (2022). Evaluation of the antibacterial inhibitory activity of chitosan nanoparticles biosynthesized by streptococcus thermophilus. *Journal of Nanostructures*, *12*(3), 675-685.

Al-Saady, A.J., Aldujaili, N.H., Banoon, S.R. & Al-Abboodi, A. (2006). Antimicrobial properties of nanoparticles in biofilms. *Revis Bionatura*, *7*(4), 71.

Al-Sultan, R.M.H., Al-Sultan, A.A., Hayawi, M.A., Aldahham, B.J., Saleh, M.Y. & Mohammed, H.A. (2017). The effect of subclinical thyroid dysfunction on B-type natriuretic peptide level. *Revis Bionatura*, *7*(2), 21.

Baliyan, S., Mukherjee, R., Priyadarshini, A., Vibhuti, A., Gupta, A., Pandey, R.P. & Chang, C.M. (2022). Determination of antioxidants by DPPH radical scavenging activity and quantitative phytochemical analysis of Ficus religiosa. *Molecules*, *27*(4), 1326.

Czerwiński, P.J., Furman, B. (2021). Reductive functionalization of amides in synthesis and for modification of bioactive compounds. *Frontiers in Chemistry*, 9, 655849.

El-Bindary, A.A., Toson, E.A., Shoueir, K.R., Aljohani, H.A. & Abo-Ser, M.M. (2020). Metal-organic frameworks as efficient materials for drug delivery: Synthesis, characterization, antioxidant, anticancer, antibacterial and molecular docking investigation. *Applied Organometallic Chemistry*, *34*(11), e5905.

Falih, I.Q., Alobeady, M.A., Banoon, S.R. & Saleh, M.Y. (2021). Role of oxidized low-density lipoprotein in human diseases: A review. *Journal of Chemical Health Risks*, 11.

Hamdoon, A.M., Saleh, M.Y. (2022). Synthesis & biological evaluation of novel series of benzo [f] indazole derivatives. *Egyptian Journal of Chemistry*, *65*(11), 305-312.

Hamdoon, A.M., Al-Iraqi, M.A. & Saleh, M.Y. (2022). Synthesis of some multi-cyclic sulfhydryl donor compounds containing 1, 2-dithiol-3-thione moiety. *Egyptian Journal of Chemistry*, *65*(3), 427-434.

Hameed, A.D., Al-Fatlawi, A.A.Y. & Al-Fatlawi, A.A.Y. (2021). Synthesis and biological activity of new sulfonamide derivatives. *International Journal of Drug Delivery Technology*, 11, 1394-1398.

Hassan, H.B. (2018). Energy gap and infrared frequencies of benzamide and di-chlorine benzamide from density functional calculations. *Research Journal of Pharmacy and Technology*, *11*(10), 4263-4266.

Hussein, A.N., Fawzi, M., Obaid, R.F., Banoon, S.R., Abood, E.S. & Ghasemian, A. (2022). Dual pharmacological targeting of Mycobacterium tuberculosis (Mtb) PKNA/PKNB: A novel approach for the selective treatment of TB illness. *Egyptian Journal of Chemistry*, *65*(12), 409-419.

Jabłońska, J., Tawfik, D.S. (2021). The evolution of oxygen-utilizing enzymes suggests early biosphere oxygenation. *Nature Ecology & Evolution*, *5*(4), 442-448.

Lawi, Z.K.K., Merza, F.A., Banoon, S.R., Jabber Al-Saady, M.A.A. & Al-Abboodi, A. (2021). Mechanisms of antioxidant actions and their role in many human diseases: A review. *Journal of Chemical Health Risks*, 11.

Liu, Z., Liu, Y., Zeng, G., Shao, B., Chen, M., Li, Z., ... & Zhong, H. (2018). Application of molecular docking for the degradation of organic pollutants in the environmental remediation: A review. *Chemosphere*, 203, 139-150.

Neubig, R.R., Spedding, M., Kenakin, T. & Christopoulos, A. (2003). International union of pharmacology committee on receptor nomenclature and drug classification. XXXVIII. Update on terms and symbols in quantitative pharmacology. *Pharmacological Reviews*, *55*(4), 597-606.

Qasim, Z.S., Abbas, K.S. (2024). Benzamine derivatives: Synthesis, characterization and biological activity study. *Chemical Problems*, *22*(4), 411-435.

Rehman, H., Qadir, A., Ali, Z., Nazir, S., Zahra, A. & Shahzady, T. G. (2017). Synthesis and characterization of novel sulfonamides derivatives and their antimicrobial, antioxidant and cytotoxicity evaluation. *Bulletin of the Chemical Society of Ethiopia*, *31*(3), 491-498.

Sadeek, G.T., Saeed, Z.F. & Saleh, M.Y. (2023). Synthesis and pharmacological profile of hydrazide compounds. *Research Journal of Pharmacy and Technology*, *16*(2), 975-982.

Saied, S.M., Mohammed, S.J., Khaleel, B.T. & Saleh, M.Y. (2021). Comparative studies between conventional techniques and green chemistry to synthesis of novel piperidinium salts ionic liquids (PBSILs). *Journal of Chemical Health Risks*, *11*(4), 451-456.

Saleh, M.Y., Al-barwari, A.S. & Ayoob, A.I. (2022). Synthesis of some novel 1, 8-naphthyridine chalcones as antibacterial agents. *Journal of Nanostructures*, *12*(3), 598-606.

Saleh, M.Y., Aldulaimi, A.K.O., Saeed, S.M. & Adhab, A.H. (2025). Palladium fabricated on Fe_3O_4 as an organic-inorganic hybrid nanocatalyst for the Suzuki and Stille coupling reactions. *Journal of Molecular Structure*, 1321, 139597.

Saleh, M.Y., Aldulaimi, A.K.O., Saeed, S.M. & Adhab, A.H. (2024). $TiFe_2O_4$@ SiO_2–SO_3H: A novel and effective catalyst for esterification reaction. *Heliyon*, *10*(4).

Salvatore, R.N., Yoon, C.H. & Jung, K.W. (2001). Synthesis of secondary amines. *Tetrahedron*, *57*(37), 7785-7811.

Sterle, M., Durcik, M., Stevenson, C.E., Henderson, S.R., Szili, P.E., Czikkely, M., ... & Zega, A. (2023). Exploring the 5-substituted 2-aminobenzothiazole-based DNA gyrase B inhibitors active against ESKAPE pathogens. *ACS Omega*, *8*(27), 24387-24395.

Tanaka, H., Tokumaru, Y., Fukui, K.I., Kuroboshi, M., Torii, S., Jutand, A. & Amatore, C. (2009). Chemo- and product-selective electrooxidation of 3-(Arylthiomethyl)-Δ^3-cephems. *Synthesis*, 20, 3449-3459. https://doi.org/10.1055/s-0029-1216972

ul Qamar, M.T., Sanz-Jimenez, P., Banoon, S.R., Zhu, X.T., Aldakheel, F.M., Almansour, N.M., ... & Ahmad, F. (2025). Computational identification of anti-cancer compounds targeting the RNA-binding domain of human FOX-1 protein (RBFOX1). *Results in Chemistry*, 13, 102004.

Wareham, L.K., Baratta, R.O., Del Buono, B.J., Schlumpf, E. & Calkins, D. J. (2024). Collagen in the central nervous system: Contributions to neurodegeneration and promise as a therapeutic target. *Molecular Neurodegeneration*, *19*(1), 11.

Yang, S., Tian, X.Y., Ma, T.Y., Dai, L., Ren, C.L., Mei, J.C., ... & Tan, C.X. (2020). Synthesis and biological activity of benzamides substituted with pyridine-linked 1, 2, 4-oxadiazole. *Molecules*, *25*(15), 3500.

Yaseen, S.N., Al-Fakhry, H.H. & Saleh, M.Y. (2025). Effects of local rosuvastatin/hyaluronan hydrogel on post-orthodontic relapse reduction in rabbits: Histological and immunohistochemical study. *Iraqi Journal of Veterinary Sciences*, *39*(1), 25-34.